



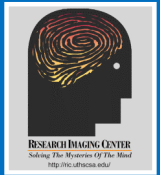
# Motor-system connectivity explored with TMS/PET and SEM

Angela R. Laird<sup>1</sup>, Jacob M. Robbins<sup>2</sup>, Karl Li<sup>1</sup>, Matthew D. Cykowski<sup>1</sup>, Shalini Narayana<sup>1</sup>, Larry R. Price<sup>3</sup>, Robert W. Laird<sup>3</sup>, Crystal Franklin<sup>1</sup>, Peter T. Fox<sup>1</sup>

<sup>1</sup>Research Imaging Center, University of Texas Health Science Center, San Antonio, Texas

<sup>2</sup>Department of Physics, Texas Lutheran University, Seguin, Texas

<sup>3</sup>Department of Educational Administration and Psychological Services, Texas State University, San Marcos, Texas



## Objective

Structural equation modeling (SEM) is a powerful tool for creating neural systems models from functional neuroimaging studies. Reducing bidirectional covariances to unidirectional paths is a significant challenge for SEM. The most common strategy is to constrain the starting model with *a priori* information, typically from anatomical connectivity studies. Because transcranial magnetic stimulation (TMS) can be applied to a discrete cortical site and propagates orthodromically from that site, it can provide unidirectional starting paths from which to model. This strategy was applied to H<sub>2</sub><sup>15</sup>O PET data acquired during image-guided TMS of the hand regions of the primary motor cortex (MI<sub>hand</sub>). The basic premise of our method was to use SEM to explore LMI<sub>hand</sub> connectivity starting only with the path connection from TMS to the stimulation site, tracking the resultant signal propagation in a stage-wise, model-expanding procedure.

## Methods

In 7 right-handed, normal volunteers, TMS was delivered via a robotic, image-guided system (Lancaster et al., 2004) to left MI<sub>hand</sub>. Stimulation was delivered at 3 intensities (75%, 100%, and 125%) relative to motor threshold (MT) and at rest (0% MT). From a meta-analysis of imaging studies of LMI<sub>hand</sub> TMS stimulation, 11 ROIs were selected: LMI<sub>hand</sub>, posterior parietal cortex (LPPC), ventral premotor cortex (LPMV), secondary somatosensory cortex (LSII, RSII), ventral lateral nucleus of the thalamus (LTHvl, RTHvl), left ventral posterolateral nucleus of the thalamus (LTHvp), SMA, cingulate gyrus (Cing), and cerebellum (RCer) (Fig. 1). TMS intensity was modeled as a variable directly modulating activation intensity at the stimulated site. All output paths from LMI<sub>hand</sub> were tested to identify the next level of nodes in the path model using the specification search of AMOS 7.0 (SPSS, Inc.). From those nodes, we continued this method of signal tracking and model testing to determine the paths from all subsequent nodes until no further paths were suggested.

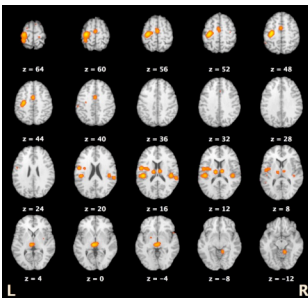


Fig. 1. TMS Meta-Analysis Results,  $P < 0.05$  (Turkeltaub et al., 2002).

## Results & Discussion

SEM began with a unidirectional input path that linked TMS intensity to LMI<sub>hand</sub>. From this path we tested 10 optional paths of signal propagation from LMI<sub>hand</sub> to all other ROIs and identified the next level of nodes: SMA, cingulate, left thalamus (LTHvl), RSII, and right cerebellum (Fig. 2a). SEM model testing continued for 2 more levels of analysis, resulting in a final neural system model of LMI<sub>hand</sub> connectivity (Fig. 2b). Overall model fit was outstanding:  $\chi^2(38) = 22.150$ ,  $P = 0.981$ , CFI = 1.0, RMSEA = 0.00, 90% CI<sub>RMSEA</sub> = 0.00-0.00. These statistics indicate little difference between the sample variance-covariance matrix and the reproduced variance-covariance matrix implied by this model. Overall, we found excellent agreement in ROI locations when comparing (1) the TMS meta-analysis and the TMS/PET data of 7 subjects, and (2) the TMS meta-analysis and a meta-analysis of voluntary finger tapping. This confirms that our method of ROI selection was successful both in identifying the nodes stimulated with TMS and that these nodes are characteristic of motor function in general. Agreement was also found in many of the paths in our final

model that are confirmed in previous human movement and grasping SEM studies and in the primate literature, specifically F1<sub>arm</sub> macaque connectivity (the homologue of MI<sub>hand</sub>).

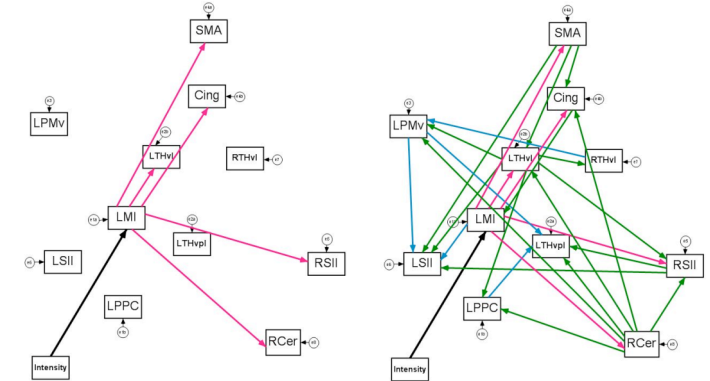


Fig. 2. (a) First-Level Paths (b) Final Path Model of LMI Connectivity. Green = 2<sup>nd</sup>-level paths; Blue = 3<sup>rd</sup>-level paths.

In order to determine the relative roles of proprioception and efference copy (Blakemore et al., 2001), we repeated our analysis in a reduced data set (no 125% MT), which were largely uncontaminated by proprioceptive feedback. The networks differed by only 3 paths (Fig. 3). Our interpretation is that Fig. 3a (with overt movement) reflects the interaction between both efference copy and proprioception in the LMI network, while Fig. 3b (no overt movement) reflects contributions from only efference copy. These conclusions agree well with previous studies that suggest modulation of efference copy occurs upstream from primary motor cortex in premotor regions (Chronicle and Glover, 2003; MacDonald and Paus, 2003). Our results also agree with previous efference copy results that found SII to be attenuated during the sensory consequences of self-generated movements (Leube et al., 2003).

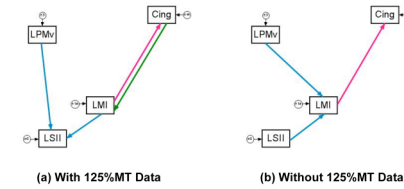


Fig. 3. Difference Between Complete and Reduced Data Models.

## Conclusions

The proposed strategy for constraining path direction by means of TMS/PET proved highly effective. We feel that this technique holds great promise for further studies of effective connectivity. However, at this point, it is unclear how generalizable our results are. We do not currently know if any of the network connections determined in our path model are similar to those during the performance of a functional task. Future studies will involve testing our model in voluntary movement data, such as finger tapping. Alternatively, it would be interesting to apply this analysis to data in which other nodes were stimulated, such as SMA, SI, SII, or premotor regions.

**References:** Blakemore et al., *Neuroreport* 12, 1879-1884, 2001; Chronicle and Glover, *Cortex* 39, 105-110, 2003; Lancaster et al., *HBM* 22, 329-340, 2004; Leube et al., *Neuroimage* 20, 2084-2090, 2003; MacDonald and Paus, *Cereb Cortex* 13, 962-967, 2003; Turkeltaub et al., *Neuroimage* 16, 765-780, 2002.

**Funding:** Human Brain Project (R01-MH074457-01A1); NIMH (R01-MH060246).